Genetic and cellular origins of histiocytic neoplasms

Kemps, P.G.

5

Clinicogenomic associations in childhood Langerhans cell histiocytosis: an international cohort study

Paul G. Kemps, Timo C.E. Zondag, Helga B. Arnardottir, Nienke Solleveld-Westerink, Jelske Borst, Eline C. Steenwijk, Demi van Egmond, Joost F. Swennenhuis, Ellen Stelloo, Irene Trambusti, Robert M. Verdijk, Carel J.M. van Noesel, Arjen H.G. Cleven, Marijn A. Vermeulen, Marco J. Koudijs, Lenka Krsková, Cynthia Hawkins, R. Maarten Egeler, Jesper Brok, Tatiana von Bahr Greenwood, Karel Svojgr, Auke Beishuizen, Jan A.M. van Laar, Ulrike Pötschger, Caroline Hutter, Elena Sieni, Milen Minkov, Oussama Abla, Tom van Wezel, Cor van den Bos, Astrid G.S. van Halteren

Blood Advances 2023;7(4):664-679.

ABSTRACT

Langerhans cell histiocytosis (LCH) is a rare neoplastic disorder caused by somatic genetic alterations in hematopoietic precursor cells differentiating into $CD1a^{+}/CD207^{+}$ histiocytes. LCH clinical manifestation is highly heterogeneous. *BRAF* and *MAP2K1* mutations account for approximately 80% of genetic driver alterations in neoplastic LCH-cells. However, their clinical associations remain incompletely understood. Here, we present an international clinicogenomic study of childhood LCH, investigating 377 patients genotyped for at least $BRAF^{V600E}$. MAPK pathway gene alterations were detected in 300 (79.6%) patients, including 191 (50.7%) with $BRAF^{V600E}$, 54 with *MAP2K1* mutations, 39 with *BRAF* exon 12 mutations, 13 with rare *BRAF* alterations, and 3 with *ARAF* or *KRAS* mutations. Our results confirm that $BRAF^{V600E}$ associates with lower age at diagnosis and higher prevalence of multisystem LCH, high-risk disease, and skin involvement. Furthermore, $BRAF^{V600E}$ appeared to correlate with a higher prevalence of central nervous system (CNS)-risk bone lesions. In contrast, *MAP2K1* mutations associated with a higher prevalence of SS-bone LCH, and *BRAF* exon 12 deletions seemed to correlate with more lung involvement. Although $BRAF^{V600E}$ correlated with reduced event-free survival (EFS) in the overall cohort, neither *BRAF* nor *MAP2K1* mutations associated with EFS when patients were stratified by disease extent. Thus, the correlation of $BRAF^{V600E}$ with inferior clinical outcome is (primarily) driven by its association with disease extents known for high rates of progression or relapse, including multisystem LCH. These findings advance our understanding of factors underlying the remarkable clinical heterogeneity of LCH, but also question the independent prognostic value of lesional $BRAF^{V600E}$ status.

INTRODUCTION

Langerhans cell histiocytosis (LCH) is a rare hematologic neoplasm characterized by the accumulation of myeloid-differentiated cells with characteristic CD1a and CD207 expression in various tissues and organs[1–3]. The disease primarily affects children, with an incidence similar to pediatric Hodgkin lymphoma[4]. LCH clinical manifestation is highly heterogeneous, ranging from self-healing skin lesions or a solitary bone lesion to a life-threatening disease involving multiple organ systems (Supplementary Figure 1)[5]. Disease extent is an established prognostic factor in pediatric LCH[6–8]. The most severe clinical form of the disease tends to affect young children (age < 2 years) and typically involves risk organs (RO), including the hematopoietic system, liver and spleen[9,10]. LCH with RO involvement is often refractory to chemotherapy and associated with an increased risk of death; therefore, it is called "high-risk LCH"[11–13]. Although overall mortality of LCH patients is low, a significant proportion of them experiences disease relapses[14] and/or develops permanent consequences, such as diabetes insipidus (DI) or neurodegenerative (ND)-LCH. Currently, the biological mechanisms underlying the heterogeneous clinical presentation and outcome of LCH remain incompletely understood.

In 2010, Rollins and colleagues discovered recurrent somatic *BRAF*^{V600E} mutations in LCH[15]. Subsequently, other groups confirmed the presence of *BRAF*^{V600E} mutations in approximately 50-60% of LCH-patients[10,16–20], and identified alternative MAPK pathway activating genetic alterations in patients without *BRAF*^{V600E} (Supplementary Figure 2)[17,21–28]. Most notably, somatic mutations in *MAP2K1* exon 2 or 3 and small insertions and/or deletions (indels) in *BRAF* exon 12 were recurrently detected[17,22–25]. Together, *BRAF* and *MAP2K1* mutations seem to account for approximately 80% of genetic driver alterations in pediatric LCH[29]. *BRAF*^{V600E}, *MAP2K1* and *BRAF* exon 12 mutations are essentially mutually exclusive[22], with only very rare cases having co-occurring mutations[30,31].

In 2016, Héritier *et al*. reported that *BRAF*^{V600E} associated with high-risk disease and increased rates of first-line therapy resistance and relapse in 315 pediatric LCH patients[10], including 173 children (54.6%) with *BRAF*^{V600E}. Since then, no study has been published with similar or more LCH patients genotyped for *BRAF*^{V600E}. Hence, their observations still need to be duly confirmed. Moreover, large cohort studies with molecular data beyond *BRAF*^{V600E} are needed to determine the clinical impact of recurrent mutations in *MAP2K1* or *BRAF* exon 12, which remain largely unknown[29]. Accordingly, here we describe an international clinicogenomic study of childhood LCH, investigating 377 patients genotyped for at least *BRAF*^{V600E}, including 300 (79.6%) patients with a detected MAPK pathway gene alteration.

MATERIALS AND METHODS

Study design

We performed an international observational cohort study of clinical associations of somatic genetic alterations in pediatric LCH. Patients were included between 2014 and 2021 in a retrospective cohort study of LCH patients in four academic children's hospitals in The Netherlands and Canada, or they were enrolled between 2013 and 2021 in the prospective LCH-IV clinical study (NCT02205762/EudraCT 2011-001699-20) in The Netherlands, Italy, Austria, Czech Republic, Sweden or Denmark. The study was performed in accordance with the Declaration of Helsinki, and ethical approval or a waiver of consent for retrospective research was obtained from the Institutional Review Boards at participating institutions. Written informed consent was obtained from patients and/or their legal representatives when required. Inclusion of patients from the LCH-IV study was approved by the Data Safety Monitoring Committee. Inclusion stopped April 30, 2021.

Patient selection and data collection

Patients were identified through registries of involved institutions. Eligibility criteria were (i) a definitive diagnosis of LCH, (ii) age at LCH diagnosis below eighteen years, and (iiia) available LCH-lesional *BRAF*^{V600E} status by PCR or sequencing through routine molecular diagnostics or (iiib) availability of formalin-fixed paraffin-embedded (FFPE) LCH tissue for molecular analysis in the specific context of this study. Diagnosis of LCH was confirmed by a combination of clinical findings and the presence of CD1a^{+} histiocytes in the lesional tissue sample(s). For patients with isolated skin disease, LCH diagnosis also required confirmation of CD207 co-expression by CD1a^{+} histiocytes, to rule out indeterminate cell histiocytosis – a diagnostic pitfall[32]. Patients enrolled in the prospective LCH-IV study were staged, treated and followed-up according to study protocol; other patients were managed according to standard-of-care. Importantly, first-line treatment and follow-up of patients were irrespective of mutational status; no patient received first-line therapy with BRAF and/or MEK inhibitors. Details of data collection are provided in the Supplementary Methods.

Disease extent was categorized according to the classification of the LCH Study Group of the Histiocyte Society[9], differentiating between single-system (SS) and multisystem (MS) disease. Within these categories, detailed subtypes were distinguished based on the type of organ(s) involved and/or the manifestation as uni- or multifocal disease. The hematopoietic system, liver and spleen were considered risk organs (RO)[9,33], and bone lesions affecting the orbital, temporal/mastoid, sphenoidal, zygomatic, or ethmoidal bones, the maxilla, paranasal sinuses, or anterior or middle cranial fossa were

considered central nervous system (CNS)-risk lesions[9,34-36]. LCH with RO involvement was termed "high-risk LCH". Event was defined as disease progression, LCH relapse or death from any cause. Disease progression was defined as (i) insufficient response and/or progression of existing LCH manifestations requiring the start or a second- or further-line of chemotherapy, targeted therapy and/or radiotherapy, or (ii) the development of new lesions in the presence of active disease. Disease relapse was defined as the development of new lesions after complete remission for prior LCH manifestations.

Molecular pathologic analysis

Molecular analysis was performed as part of routine diagnostics and/or in the specific context of this study. Importantly, none of the tissue samples were analyzed by BRAF-VE1 immunohistochemistry alone. For (additional) molecular analysis performed in the context of this study, manual microdissection of LCH-lesional FFPE tissue sections was performed based on a CD1a stained reference slide to obtain representative tissue parts enriched for neoplastic LCH-cells[37], thereby increasing the success rate of mutation detection[38]. Automated DNA isolation from the microdissected tissue fragments and *BRAF*^{V600E} allele-specific real-time PCR and/or droplet digital PCR were performed as previously described[39-41]. When possible, cases without *BRAF*^{V600E} were further analyzed using Sanger sequencing and/or a custom-designed AmpliSeq next-generation-sequencing (NGS) panel containing primers to detect mutations in *MAP2K1* (NM_002755.3) exon 2-3 and *BRAF* (NM_004333.6) exon 12+15, as well as in *ARAF*, *MAP3K1*, *N/KRAS* and many other cancer-associated genes (Supplementary Methods)[42]. Finally, a small proportion of *BRAF*^{V600E} negative patients was analyzed for alternative *BRAF* alterations by FFPE-targeted locus capture (FFPE-TLC) NGS[43,44] – a DNA-based technique able to identify both small variants (e.g. single nucleotide variants or small indels) and structural variants (e.g. gene rearrangements). Details are available in the Supplementary Methods.

Statistical analysis

Comparisons of (sub)groups were performed using the two-sided Mann-Whitney U or Kruskal-Wallis test for continuous data and two-sided Fisher's or Fisher-Freeman-Halton exact test for categorical data. In general, threshold for significance was $P < 0.05$; however, in univariable analysis of LCH presentation according to mutational status $P < 0.00125$ was considered statistically significant (Bonferroni correction for multiple testing)[10]. In addition to significant results, findings insignificant after Bonferroni correction but with P values < 0.05 were highlighted. These represent potential associations, but without sufficient statistical evidence in this study, and will require further careful evaluation to determine their potential clinical relevance. Variables

significant after correction were included in a multivariable binary logistic regression analysis to identify the factor(s) most associated with *BRAF*^{V600E} after adjustment for the other variables. For hierarchical categorical variables (e.g. bone – bone subtypes), the primary variable was considered for inclusion (e.g. bone). Because risk organ involvement was restricted to MS-LCH, liver and hematopoietic system involvement – both significant in univariable analysis – were not included as independent variables, but instead MS-RO+ LCH was added as disease extent category to the regression model. Univariable survival analyses were performed using the Kaplan-Meier method, and survival curves were compared using the log-rank test. Event-free survival (EFS) was defined as the time from diagnosis until the first event or – for cases without an event – the date of last follow-up. To investigate how much of the effect of *BRAF*^{V600E} on EFS was mediated by disease extent, univariable survival analyses were stratified by disease extent and multivariable survival analysis was performed using Cox regression. Median follow-up was estimated using the reverse Kaplan-Meier method[45]. Incidences of DI, ND-LCH, specific sites of disease, chemotherapy, and second-line systemic therapy were indicated by proportions[10], because of incomplete time-to-event data for cumulative incidence calculations. Statistical analyses were performed using Graphpad Prism 9.0.1 or IBM SPSS Statistics 25.

RESULTS

A total of 377 patients with childhood LCH and available *BRAF*^{V600E} status were included. This cohort comprised 198 (52.5%) patients from the prospective LCH-IV study and 179 (47.5%) patients from a Dutch-Canadian retrospective study, with comparable clinical characteristics (Supplementary Table 1). The combined cohort comprised 222 (58.9%) males and 155 (41.1%) females. Median age at diagnosis was 3.6 years (range 0.0 – 17.9 years). Patients could be classified into 288 (76.4%) patients with SS-LCH and 89 (23.6%) patients with MS-LCH. Patients with SS-LCH could be categorized into 184 patients with unifocal bone disease (SS-UFB), 64 patients with multifocal bone disease (SS-MFB), 32 patients with isolated skin disease (SS-skin), and 8 patients with isolated involvement of another organ system, including the lungs (*N* = 3), lymph nodes (*N* = 3), CNS (*N* = 1) or soft tissue (*N* = 1). Patients with MS-LCH could be divided into 55 patients without risk organ involvement (MS-RO-) and 34 patients with risk organ involvement (MS-RO+ or high-risk LCH).

MAPK pathway gene alterations were detected in 300/377 (79.6%) patients, including 191 (50.7%) with *BRAF*^{V600E} (Table 1). In the subgroup without *BRAF*^{V600E}, *MAP2K1* mutations were identified in 54 patients and *BRAF* exon 12 indels were detected in 39

children (Table 2). *MAP2K1* mutations occurred in exon 2 in 36/54 (66.7%) patients and in exon 3 in 18/54 (33.3%) patients. *BRAF* exon 12 indels included small in-frame deletions at the beginning of exon 12 affecting the β3-αC loop in 27/39 (69.2%) patients and in-frame insertions of nine nucleotides at the end of exon 12 affecting the αC-β4 loop in 12/39 (30.8%) patients[25,46-48]. In the remaining *BRAF*^{V600E} negative patients, *BRAF* exon 15 mutations other than *BRAF*^{V600E} (*N*=10), *BRAF* fusions (*N*=3), *ARAF* mutations (*N*=2), and a *KRAS* mutation (*N*=1) were detected (Supplementary Table 2).

Table 1. Clinical characteristics according to *BRAF*^{V600E} status

	***BRAF*^{V600E} positive**	***BRAF*^{V600E} negative**	**OR (95% CI)**	***P* value**	
Patients	191	186			
Age at diagnosis, median (range)	2.6 years (0.0 – 17.6)	5.7 years (0.0 – 17.9)	N/A	<0.001	**
Age <3 years	105 (55.0%)	66 (35.5%)	2.22 (1.47-3.36)	<0.001	**
Age ≥3 years	86 (45.0%)	120 (64.5%)			
Sex					
Male	113 (59.2%)	109 (58.6%)	1.02 (0.68-1.54)	0.92	
Female	78 (40.8%)	77 (41.4%)			
Disease extent at diagnosis					
Multisystem	64 (33.5%)	25 (13.4%)	3.25 (1.93-5.45)	<0.001	**
Single system	127 (66.5%)	161 (86.6%)			
Detailed subtype[$]					
MS, RO+	27 (14.1%)	7 (3.8%)	4.21 (1.79-9.93)	<0.001	**
MS, RO-	37 (19.4%)	18 (9.7%)	2.24 (1.23-4.10)	0.009	*
SS, bone	109 (57.1%)	139 (74.7%)	0.45 (0.29-0.70)	<0.001	**
SS, UFB	87 (45.5%)	97 (52.2%)	0.77 (0.51-1.15)	0.22	
SS, UFB, CNS-risk[$$]	16 (8.4%)	19 (10.2%)	0.80 (0.40-1.62)	0.60	
SS, MFB	22 (11.5%)	42 (22.6%)	0.45 (0.26-0.78)	0.006	*
SS, skin	18 (9.4%)	14 (7.5%)	1.28 (0.62-2.65)	0.58	
SS, other	0 (0.0%)	8[§§] (4.3%)	N/A	0.003	*
Disease site(s) at diagnosis					
Bone	157 (82.2%)	159 (85.5%)	0.78 (0.45-1.36)	0.41	
Multifocal bone lesions	56 (29.3%)	55 (29.6%)	0.99 (0.63-1.54)	1	
CNS-risk bone lesion(s)[$$]	64 (33.5%)	40 (21.5%)	1.84 (1.16-2.92)	0.011	*
Spinal column lesion(s)	18 (9.4%)	28 (15.1%)	0.59 (0.31-1.10)	0.12	

Table 1. Clinical characteristics according to *BRAF*^{V600E} status (continued)

	***BRAF*^{V600E} positive**	***BRAF*^{V600E} negative**	**OR (95% CI)**	***P* value**	
Skin	69 (36.1%)	24 (12.9%)	3.82 (2.27-6.43)	<0.001	**
Liver[#]	24 (12.6%)	5 (2.7%)	5.20 (1.94-13.95)	<0.001	**
Hematopoietic system[#]	19 (9.9%)	3 (1.6%)	6.74 (1.96-23.18)	0.001	**
Spleen[#]	15 (7.9%)	4 (2.2%)	3.88 (1.26-11.91)	0.017	*
Lymph node	17 (8.9%)	17 (9.1%)	0.97 (0.48-1.97)	1	
Lung	10 (5.2%)	14 (7.5%)	0.68 (0.29-1.57)	0.40	
Central nervous system[##]	8 (4.2%)	4 (2.2%)	1.99 (0.59-6.72)	0.38	
Gastrointestinal tract	7 (3.7%)	0 (0.0%)	N/A	0.015	*
Follow-up, median (range)	4.0 years (0.0 – 38.8)	3.8 years (0.0 – 36.0)	N/A	0.61[†]	
Permanent consequences developed during follow-up					
Diabetes insipidus	23 (12.0%)	14 (7.5%)	1.68 (0.84-3.38)	0.17	
Neurodegenerative LCH[§]	5 (2.6%)	0 (0.0%)	N/A	0.06	
Death	4	4	N/A	0.97†	

Symbols: [$] Fisher's exact tests comparing patients with vs. without a disease extent subtype are shown. Fisher-Freeman-Halton exact test comparing proportions in all different subgroups (a contingency table larger than 2x2) is not shown, but was significant (*P* <0.001). [$$] Bone lesions affecting the orbital, temporal/mastoid, sphenoidal, zygomatic, or ethmoidal bones, the maxilla, paranasal sinuses, or anterior or middle cranial fossa. [#] These organs are considered risk organs. [##] Given that the posterior pituitary and pituitary stalk are direct extensions of the hypothalamus, pituitary tumors are classified as CNS involvement. All twelve patients with CNS involvement at diagnosis had tumorous lesions, e.g. pituitary stalk lesions. [§] Only patients with both clinical and radiologic neurodegenerative LCH are reported. [§§] These eight patients comprised three patients with SS-lung LCH, three patients with SS-lymph node LCH, and single cases with SS-soft tissue or (tumorous) SS-CNS disease. [†] Obtained with the log-rank test. * *P* <0.05. ** *P* <0.00125 (Bonferroni correction for multiple testing; tests are shown in this table and Supplementary Table 3). Abbreviations: SS, single-system; UFB, unifocal bone; CNS, central nervous system; MFB, multifocal bone; MS, multisystem; RO, risk organ; N/A, not available.

Table 2. Clinical characteristics of patients with *MAP2K1* or *BRAF* exon 12 mutations

	MAP2K1 mutated			*BRAF* exon 12 mutated		
	***MAP2K1* exon 2**	***MAP2K1* exon 3**	**All patients**	**In-frame deletions**	**In-frame insertions**	**All patients**
Patients	36	18	54	27	12	39
Age at diagnosis, median (range)	2.7 years (0.0-15.1)	8.3 years (1.7-17.1)	4.8 years (0.0 – 17.1)	3.4 years (0.2-17.9)	6.2 years (0.5-14.4)	5.9 years (0.2 - 17.9)
Age <3 years	19 (52.8%)	1 (5.6%)	20 (37.0%)	12 (44.4%)	3 (25.0%)	15 (38.5%)
Age ≥3 years	17 (47.2%)	17 (94.4%)	34 (63.0%)	15 (55.6%)	9 (75.0%)	24 (61.5%)
Sex						
Male	23 (63.9%)	10 (55.6%)	33 (61.1%)	16 (59.3%)	5 (41.7%)	21 (53.8%)
Female	13 (36.1%)	8 (44.4%)	21 (38.9%)	11 (40.7%)	7 (58.3%)	18 (46.2%)
Disease extent at diagnosis						
Multisystem	3 (8.3%)	1 (5.6%)	4 (7.4%)	7 (25.9%)	1 (8.3%)	8 (20.5%)
Single system	33 (91.7%)	17 (94.4%)	50 (92.6%)	20 (74.1%)	11 (91.7%)	31 (79.5%)
Detailed subtype						
MS, RO+	1 (2.8%)	0 (0.0%)	1 (1.9%)	3 (11.1%)	0 (0.0%)	3 (7.7%)
MS, RO-	2 (5.6%)	1 (5.6%)	3 (5.6%)	4 (14.8%)	1 (8.3%)	5 (12.8%)
SS, bone	30 (83.3%)	16 (88.9%)	46 (85.2%)	15 (55.6%)	11 (91.7%)	26 (66.7%)
SS, UFB	22 (61.1%)	13 (72.2%)	35 (64.8%)	11 (40.7%)	8 (66.7%)	19 (48.7%)
SS, UFB, CNS-risk	4 (11.1%)	1 (5.6%)	5 (9.3%)	4 (14.8%)	2 (16.7%)	6 (15.4%)
SS, MFB	8 (22.2%)	3 (16.7%)	11 (20.4%)	4 (14.8%)	3 (25.0%)	7 (17.9%)
SS, skin	3 (8.3%)	0 (0.0%)	3 (5.6%)	2 (7.4%)	0 (0.0%)	2 (5.1%)
SS, other	0 (0.0%)	1 (5.6%)	1 (1.9%)	3 (11.1%)	0 (0.0%)	3 (7.7%)

Table 2. Clinical characteristics of patients with *MAP2K1* or *BRAF* exon 12 mutations (continued)

	MAP2K1 mutated			*BRAF* exon 12 mutated		
	***MAP2K1* exon 2**	***MAP2K1* exon 3**	**All patients**	**In-frame deletions**	**In-frame insertions**	**All patients**
Disease site(s) at diagnosis						
Bone	33 (91.7%)	17 (94.4%)	50 (92.6%)	20 (74.1%)	12 (100%)	32 (82.1%)
Multifocal bone lesions	11 (30.6%)	3 (16.7%)	14 (25.9%)	7 (25.9%)	3 (25.0%)	10 (25.6%)
CNS-risk bone lesion(s)	8 (22.2%)	1 (5.6%)	9 (16.7%)	8 (29.6%)	3 (25.0%)	11 (28.2%)
Spinal column lesion(s)	6 (16.7%)	2 (11.1%)	8 (14.8%)	5 (18.5%)	2 (16.7%)	7 (17.9%)
Skin	5 (13.9%)	0 (0.0%)	5 (9.3%)	6 (22.2%)	0 (0.0%)	6 (15.4%)
Liver	0 (0.0%)	0 (0.0%)	0 (0.0%)	3 (11.1%)	0 (0.0%)	3 (7.7%)
Hematopoietic system	1 (2.8%)	0 (0.0%)	1 (1.9%)	1 (3.7%)	0 (0.0%)	1 (2.6%)
Spleen	0 (0.0%)	0 (0%)	0 (0.0%)	2 (7.4%)	0 (0.0%)	2 (5.1%)
Lymph node	2 (5.6%)	2 (11.1%)	4 (7.4%)	4 (14.8%)	1 (8.3%)	5 (12.8%)
Lung	1 (2.8%)	0 (0.0%)	1 (1.9%)	6 (22.2%)	0 (0.0%)	6 (15.4%)
CNS	1 (2.8%)	0 (0.0%)	1 (1.9%)	1 (3.7%)	0 (0.0%)	1 (2.6%)
Follow-up, median (range)	2.7 years (0.2-15.2)	4.3 years (1.4-30.4)	3.7 years (0.2 - 30.4)	6.3 years (0.4-27.0)	3.5 years (0.7-9.4)	5.3 years (0.4 - 27.0)
Permanent consequences during follow-up						
Diabetes insipidus	1 (2.8%)	1 (5.6%)	2 (3.7%)	5 (18.5%)	0 (0.0%)	5 (12.8%)
Death	2	0	2	2	0	2

BRAF^{V600E} status in relation to clinical presentation

BRAF^{V600E} correlated with demographic characteristics, disease extent and specific sites of disease at diagnosis (Figure 1; Table 1; Supplementary Table 3). Patients with *BRAF*^{V600E} were significantly younger than patients without *BRAF*^{V600E} (median age 2.6 years vs. 5.7 years; P <0.001). In addition, *BRAF*^{V600E} positive patients more often had MS-LCH (33.5% vs. 13.4%; P <0.001; Figure 1A) and high-risk disease (14.1% vs. 3.8%; P <0.001). Regarding sites of disease, *BRAF*^{V600E} significantly associated with more involvement of the skin (P < 0.001), liver (P < 0.001) and hematopoietic system (P = 0.001), and with less involvement of the upper extremity bones (P = 0.001; Figure 1B). Within SS-skin LCH, *BRAF*^{V600E} was significantly associated with multifocal skin involvement (P = 0.001; Figure 1C).

Concerning potential associations, *BRAF*^{V600E} seemed associated with less SS-MFB disease (P = 0.006; Figure 1A). Furthermore, *BRAF*^{V600E} appeared to correlate with a higher prevalence of spleen involvement (P = 0.017), gastrointestinal involvement (P = 0.015; Table 1), and CNS-risk bone lesions (P = 0.011; Figure 1B). When analyzing sites of disease during entire follow-up – including at LCH progression and/or relapse, these potential associations remained apparent (Supplementary Figure 3; Supplementary Table 4).

In multivariable analysis with age, disease extent (categorized as SS/MS-RO-/MS-RO+ LCH) and skin involvement as independent variables (Supplementary Table 5A), *BRAF*^{V600E} was significantly associated with skin involvement (OR 2.23, 95% CI 1.16-4.29, P = 0.017). However, odds ratio was highest for MS-RO+ disease extent (OR 2.54, 95% CI 0.99-6.54, P = 0.05). In a regression model with age, multisystem disease (irrespective of RO status) and skin involvement as independent variables, *BRAF*^{V600E} was significantly associated with both multisystem disease and skin involvement (Supplementary Table 5B).

MAP2K1 and *BRAF* exon 12 mutations in relation to clinical presentation

MAP2K1 mutations also correlated with clinical features at diagnosis (Figure 2; Supplementary Table 6). Compared to children with *BRAF*^{V600E}, patients with *MAP2K1* mutations had significantly more SS-bone LCH (85.2% vs. 57.1%; P <0.001; Figure 2D), and less MS-LCH (7.4% vs. 33.5%; P <0.001; Figure 2E) and skin involvement (9.3% vs. 36.1%; P <0.001; Figure 2G). *MAP2K1* mutations also appeared to correlate with more SS-bone disease when compared to *BRAF* exon 12 mutations (P = 0.045; Figure 2D); particularly compared to *BRAF* exon 12 deletions affecting the β3-αC loop (P = 0.006; Supplementary Figure 4B). Regarding subtypes of bone involvement, *MAP2K1* mutated patients had the lowest prevalence of CNS-risk bone lesions, despite having the most bone involvement (Figure 2F). Children with *MAP2K1* mutations did have highest prevalence of bone lesions in the upper extremities and/or shoulder girdle (Supplementary Figure 5). Regarding demographic characteristics, *MAP2K1* mutations appeared to correlate with older age at diagnosis when compared to *BRAF*^{V600E} (P = 0.011; Figure 2B).

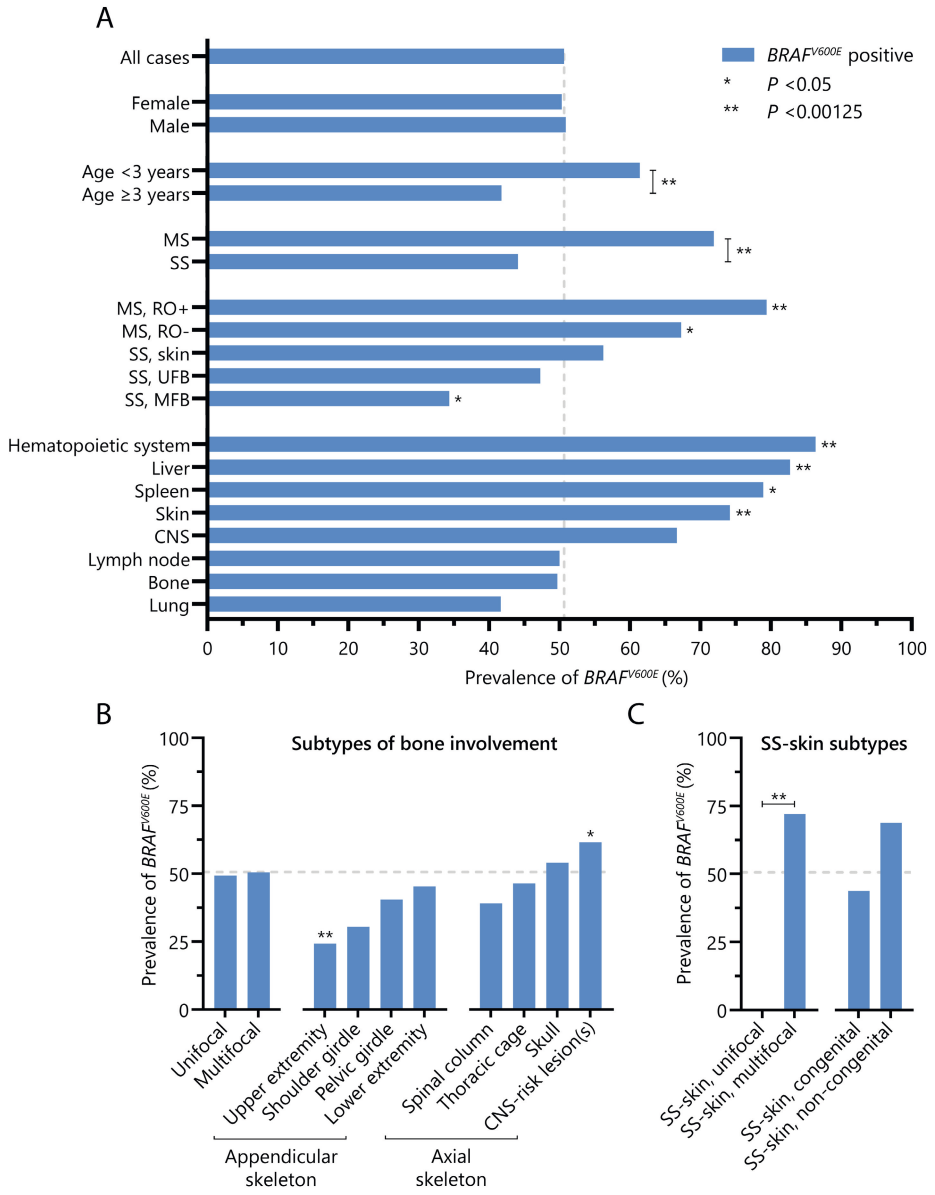

Figure 1. Clinical features at LCH diagnosis according to *BRAF*^{V600E} status. (A) Prevalence of *BRAF*^{V600E} in patients with specific clinical characteristics at LCH diagnosis. **(B)** Prevalence of *BRAF*^{V600E} in patients with specific types of bone involvement at diagnosis. This figure depicts all patients with osseous lesions, irrespective of single- or multisystemic disease extent. Bones are grouped according to the classification used by the National Cancer Institute. Upper extremity: humerus, radius, ulna, carpals, metacarpals, phalanges. Shoulder girdle: clavicle, scapula. Pelvic girdle: coxal, innominate and hip bones (incl. ilium, ischium, acetabulum, and pubis). Lower extremity: femur, tibia, fibula, patella, tarsals, metatarsals, phalanges. Spinal column: cervical, thoracic and lumbar vertebrae, sacrum, coccyx. Thoracic cage: ribs and sternum. CNS-risk lesions are bone

lesions affecting the orbital, temporal/mastoid, sphenoidal, zygomatic, or ethmoidal bones, the maxilla, paranasal sinuses, or anterior or middle cranial fossa, according to LCH Study Group definitions[9,34-36]. **(C)** Prevalence of *BRAF*^{V600E} in patients with specific presentations of single-system skin LCH at diagnosis. Numbers of patients are provided in Table 1 and Supplementary Table 3. Dashed lines indicate the prevalence of *BRAF*^{V600E} in all cases (51%). Statistical tests with *P* values <0.05 are shown. Symbols: **, *P* <0.00125; *, *P* <0.05. Abbreviations: MS, multisystem; SS, single-system; RO, risk organ; UFB, unifocal bone; MFB, multifocal bone; CNS, central nervous system.

Similar to what was observed for *MAP2K1* mutations, *BRAF* exon 12 indels seemed associated with older age at diagnosis (*P* = 0.049; Figure 2B) and less skin involvement (*P* = 0.014; Figure 2G) when compared to *BRAF*^{V600E}. Furthermore, *BRAF* exon 12 mutations appeared to correlate with a higher prevalence of lung involvement when compared to *BRAF*^{V600E} (*P* = 0.035) or *MAP2K1* mutations (*P* = 0.020; Figure 2H). Pulmonary involvement was particularly frequent in patients with *BRAF* exon 12 deletions affecting the β3-αC loop (6/27, 22.2%; Supplementary Figure 4F). Notably, *BRAF* exon 12 deletions were also detected in 3/7 (43%) patients with thymic involvement[49–51]; the other four patients had alternative *BRAF* alterations (Supplementary Figure 6).

BRAF^{V600E} status in relation to clinical outcome

Follow-up was similar for *BRAF*^{V600E} positive and negative patients (median 4.0 years vs. 3.8 years; *P* = 0.61). In the overall cohort, children with *BRAF*^{V600E} had significantly reduced EFS (5-year EFS 54.1%, SE ±4.4% vs. 59.9%, SE ±4.4%; *P* = 0.038; Figure 3A), but not reduced overall survival (Supplementary Figure 7). *BRAF*^{V600E} mutated patients also more frequently received second-line systemic therapy (29.1% vs. 15.8%; Supplementary Table 7). When patients were stratified by disease extent, however, *BRAF*^{V600E} no longer associated with outcome parameters like EFS (Figure 3B-D). *BRAF*^{V600E} mutated children particularly had noninferior EFS in the subgroups of patients with SS-UFB disease (Figure 3D) or SS-MFB LCH (Supplementary Figure 8) – representing almost two-thirds (66%) of all patients in our cohort. Additionally, disease extent but not lesional *BRAF*^{V600E} status was associated with EFS in multivariable survival analysis of the overall cohort (*BRAF*^{V600E} HR 1.08, 95% CI 0.75-1.55, *P* = 0.67; Supplementary Table 8).

MAP2K1 and *BRAF* exon 12 mutations in relation to clinical outcome

Follow-up was similar for *BRAF*^{V600E}, *MAP2K1* and *BRAF* exon 12 mutated patients (median 4.0 years vs. 3.7 years vs. 5.3 years, respectively; *P* = 0.87). No significant differences in EFS were observed between the three molecular subgroups – particularly after patient stratification by disease extent (Figure 3E-F; Supplementary Figures 8-9). Incidence of DI was similar among children with *BRAF*^{V600E} or *BRAF* exon 12 mutations (12.0% vs. 12.8%), and higher than among children with *MAP2K1* mutations (3.7%) – although not statistically significant (Tables 1-2; Supplementary Table 6).

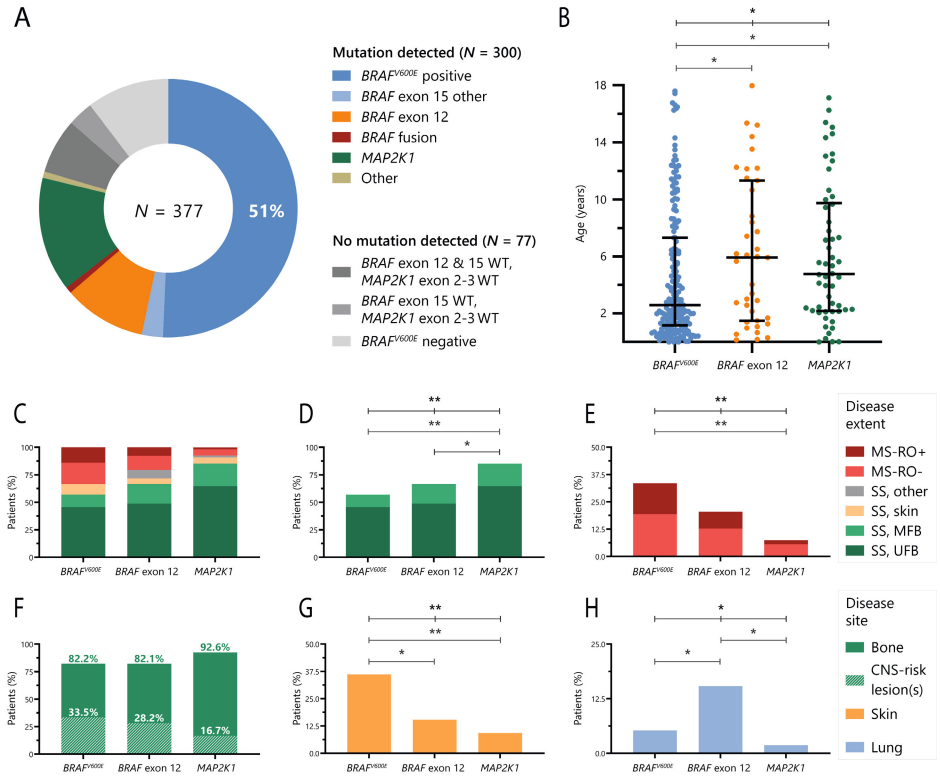

Figure 2. Clinical features at LCH diagnosis of children with *BRAF*^{V600E}, *BRAF* exon 12 or *MAP2K1* mutations. (A) Pie chart showing the mutational status of the 377 patients from our cohort. **(B)** Dot plot showing age at diagnosis of patients with *BRAF*^{V600E}, *BRAF* exon 12 or *MAP2K1* mutations. Error bars depict medians with interquartile ranges. **(C-E)** Bar charts depicting the percentage of patients with *BRAF*^{V600E}, *BRAF* exon 12 or *MAP2K1* mutations having specific disease extents at LCH diagnosis. Statistical comparisons were performed for SS-bone disease in panel D and multisystem disease in panel E. **(F-H)** Bar charts depicting the percentage of patients with *BRAF*^{V600E}, *BRAF* exon 12 or *MAP2K1* mutations having specific disease sites at LCH diagnosis. Statistical tests with *P* values <0.05 are depicted. Numbers of patients are provided in Tables 1-2. Symbols: **, *P* <0.00125; *, *P* <0.05. New abbreviation: WT, wildtype.

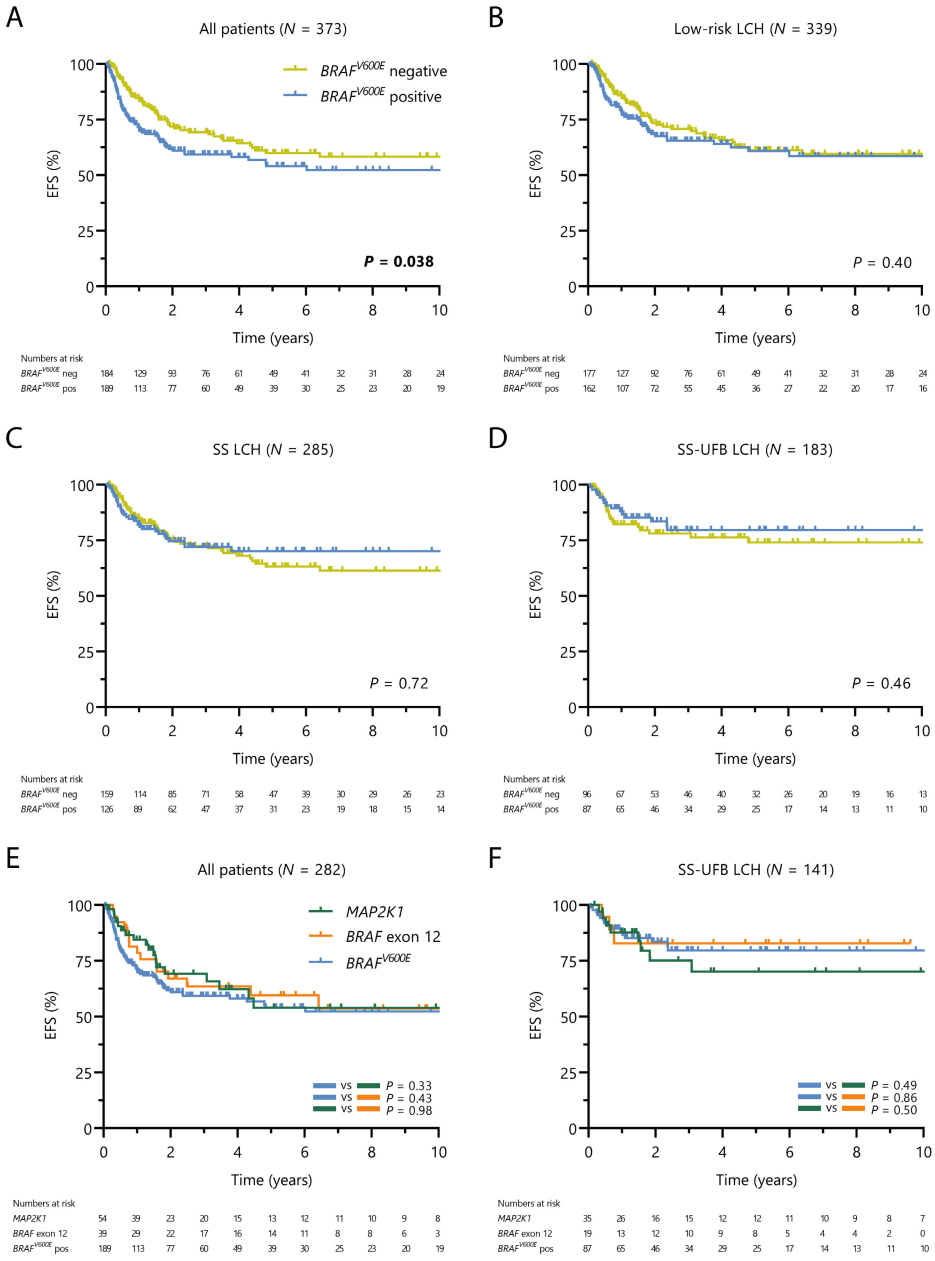

Figure 3. Clinical outcome of pediatric LCH patients according to mutational status and disease extent. (A-D) Kaplan-Meier curves showing event-free survival (EFS) according to lesional *BRAF*^{V600E} status for all 373 patients (panel A), 339 patients with low-risk LCH (panel B), 285 patients with single-system LCH (panel C) or 183 patients with single-system unifocal bone LCH at diagnosis. Patients with low-risk LCH comprise all patients except those with high-risk (= MS-RO+) disease. **(E-F)** Kaplan-Meier curves showing EFS of patients with *BRAF*^{V600E}, *BRAF* exon 12 or *MAP2K1* mutations. Curves are shown for all 282 patients (panel E) and for 141 patients with single-system unifocal bone LCH at diagnosis. Four patients without clinical follow-up were not included in these survival analyses.

Clinical features of LCH patients with alternative MAPK pathway gene alterations
Rare MAPK pathway gene alterations were identified in sixteen *BRAF*^{V600E} negative patients (Supplementary Tables 2 and 11). Ten children had a *BRAF* exon 15 mutation other than *BRAF*^{V600E}, including six with a *BRAF*^{V600D} mutation[52] and single cases with a *BRAF* p.T599_V600insEAT, *BRAF* p.T599_V600insEKST, *BRAF* p.V600_R603delinsEKSQ, or *BRAF* p.V600_W604delinsESRG mutation. All six patients with *BRAF*^{V600D} had SS-bone LCH (either UFB or MFB); none of them developed disease in another organ system during follow-up (median 4.7 years; range 0.6 – 12.6 years). However, several *BRAF*^{V600D} mutated patients had uncommon abscess-like soft tissue extension through the skin (Figure 4E; Supplementary Table 2)[53]. The patient with the *BRAF* p.V600_R603delinsEKSQ mutation had MS-RO+ disease and required second- and third-line chemotherapy. *BRAF* fusions were identified in three patients using FFPE-TLC NGS (Figure 4A-D; Supplementary Figure 10)[44]. All three cases had different *BRAF* fusion partners – including *TMEM106B*, *DOCK8* and *BICD2*. Two of three *BRAF*-rearranged patients had SS-bone LCH without progression or relapse during their follow-up (5.4 or 27.5 years); the remaining patient with a *BICD2*::*BRAF* fusion had MS-RO- disease with uncommon large tumors in both lungs (Figure 4G) – instead of small nodules and cysts typical for pulmonary LCH[54–56]. This patient had progressive disease despite two lines of chemotherapy and recently received MEK inhibition (trametinib) with a complete metabolic response after six months of treatment. The *ARAF* and *KRAS* mutations were confined to patients with SS-bone LCH.

Additional MAPK pathway gene alterations were identified in three *BRAF*^{V600E} positive cases, including one previously reported patient with a *MAP3K1* mutation[24]. The other two cases had an additional *BRAF* p.R603Q mutation, previously also reported in another child with *BRAF*^{V600E} mutated LCH[17]. One of our patients had SS-UFB LCH with multiple bone relapses during follow-up – requiring multiple lines of chemotherapy. The other child had MS-RO+ disease and required second-line chemotherapy with cladribine because of progression of lung lesions. Eventually, all patients reached complete remission (Supplementary Table 2).

DISCUSSION

Through an international collaborative effort, we present here a large clinicogenomic study of childhood LCH. We confirm findings of previous research, most notably by Héritier *et al.*[10], but also reveal new associations of *BRAF* and *MAP2K1* mutations with clinical features at presentation (Table 3). In addition, we highlight that lesional *BRAF*^{V600E} status did not correlate with inferior clinical outcome after patient stratification by disease extent – a prognostic factor known for decades[6–8].

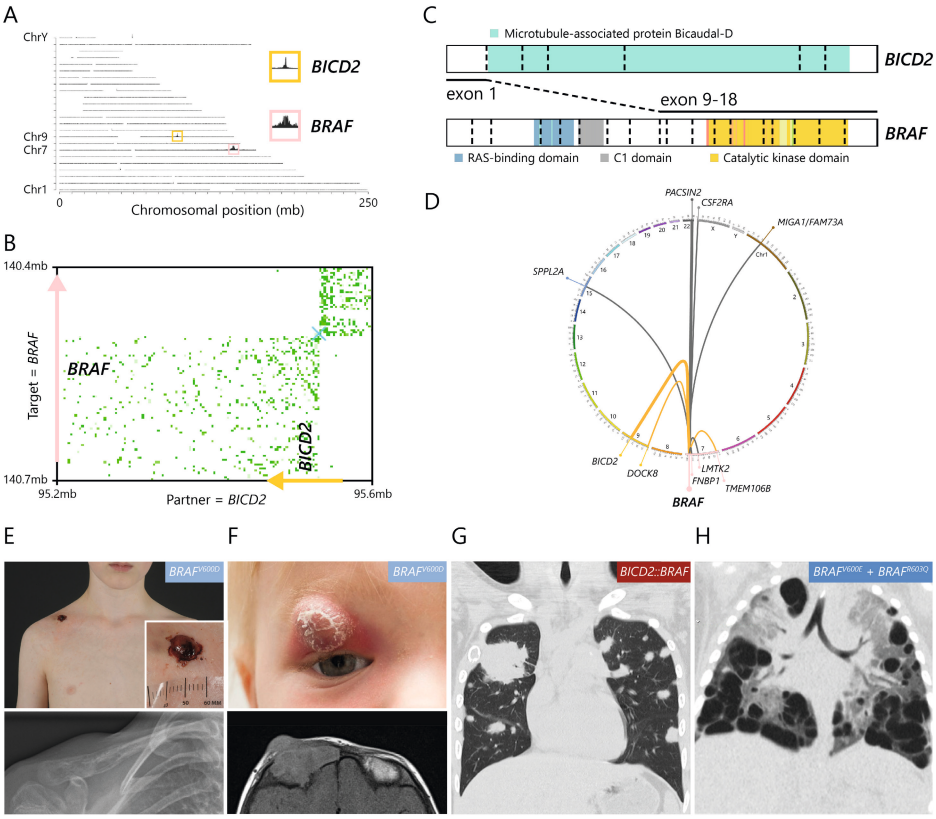

Figure 4. Molecular and clinical findings in patients with rare *BRAF* alterations. (A) Genome-wide coverage of fragments retrieved from a FFPE-TLC experiment targeting *BRAF* on a FFPE tissue sample from a patient from our cohort. A rearranged region to the *BRAF* gene (pink box) on chromosome 7 was identified by the concentration of fragments clustered around the *BICD2* gene (yellow box) on chromosome 9. **(B)** Butterfly plot uncovering the reciprocal *BICD2*::*BRAF* rearrangement. Proximity-ligation products between the target gene (*BRAF*) and rearrangement partner (*BICD2*) are depicted in green. Strand directions are indicated by arrows. See Supplementary Figure 10 for details about FFPE-TLC technology. **(C)** Illustration of the identified *BICD2*::*BRAF* fusion, made with ProteinPaint software[83]. **(D)** Circos plot depicting the three distinct *BRAF* rearrangements identified in patients from our cohort in orange, as well as other *BRAF* rearrangements previously identified in LCH patients in grey[17,25,86-88]. **(E)** Clinical and conventional radiography images of a patient from our cohort with *BRAF*^{V600D} mutated SS-UFB LCH, who had a single osteolytic lesion in the right clavicle with remarkable abscess-like soft tissue extension through the skin. **(F)** Clinical and magnetic resonance imaging (MRI) images of a patient from our cohort with *BRAF*^{V600D} mutated SS-MFB LCH, who had a relapse of multifocal bone disease with a remarkable orbital lesion with clear skin changes. **(G)** Coronal image of a chest computed tomography (CT) scan showing atypical pulmonary lesions in the patient with a *BICD2*::*BRAF* fusion. Shown are multiple solid nodules in both lungs, including a very large tumor in the right upper lobe measuring 55 x 18 x 15 mm. A biopsy of this tumor excluded co-occurrence of lymphoma or another disease and revealed clusters of CD1a^{+} CD207^{+} cells, compatible with LCH. **(H)** Coronal image of a chest CT scan showing many large cystic lung lesions in a child with high-risk LCH harboring both *BRAF*^{V600E} and *BRAF*^{R603Q} mutations.

Table 3. Summary of key findings

Mutational status in relation to clinical presentation					
Significant associations ($P < 0.00125$)			**Potential associations ($P \geq 0.00125 - P < 0.05$)**		
BRAF^{V600E}	↑ Multisystem disease	Confirming prior findings[10]	*BRAF*^{V600E}	↑ CNS-risk bone involvement	New findings
	↑ Multifocal SS-skin disease			↑ Gastrointestinal involvement	
	↑ Risk organ involvement			↓ SS-MFB disease	
	↑ Skin involvement		*BRAF* exon 12	↑ Lung involvement	
	↓ Age at diagnosis				
	↓ Upper extremity bone involvement	New findings			
MAP2K1	↑ SS-bone disease				

Mutational status in relation to clinical outcome					
Significant associations ($P < 0.05$)			**No evidence for associations ($P \geq 0.05$)**		
BRAF^{V600E}	↓ EFS when analyzing the overall cohort	Confirming prior findings[10]	*BRAF*^{V600E}	Outcome in clinical subgroups, e.g. SS-UFB	Highlighted negative findings
	↑ 2nd line systemic therapy (overall cohort)		*BRAF* exon 12 *MAP2K1*	Outcome in overall cohort and subgroups	

For associations of *BRAF*^{V600E}, *BRAF*^{V600E} positive ($N = 191$) vs. *BRAF*^{V600E} negative ($N = 186$) patients were compared. For associations of *MAP2K1* or *BRAF* exon 12 mutations, assignment is based on the statistical comparison of *MAP2K1* mutated patients ($N = 54$) or *BRAF* exon 12 mutated patients ($N = 39$) with *BRAF*^{V600E} positive patients, respectively. Associations of *MAP2K1* or *BRAF* exon 12 mutations required 1) a difference with *BRAF*^{V600E} positive patients resulting in a Fisher's Exact test P value <0.05 (for potential associations) or <0.00125 (for significant associations), and 2) a difference between *MAP2K1* and *BRAF* exon 12 mutated patients resulting in a Fisher's Exact test P value <0.05.

Regarding *BRAF*^{V600E}, our study points at a potential association with a higher prevalence of gastrointestinal involvement. Interestingly, gastrointestinal involvement was recently shown to provide additive unfavorable prognostic impact in patients with high-risk LCH[57]. Together, these data further support that *BRAF*^{V600E} associates with the most severe clinical presentations of pediatric LCH. *BRAF*^{V600E} also seemed more prevalent in patients with CNS-risk bone lesions; thus, *BRAF*^{V600E} now appears to associate with all disease characteristics known to correlate with clinical ND-LCH, including multisystem disease, skin and pituitary involvement, and CNS-risk bone lesions[10,34,35,58]. Accordingly,

all five patients with clinical ND-LCH in our cohort harbored *BRAF*^{V600E} (Table 1) and had at least one of these disease characteristics. Although we confirm that *BRAF*^{V600E} correlates with reduced event-free survival in the overall cohort[10], we show that this is (primarily) driven by the association of *BRAF*^{V600E} with disease extents known for high rates of progression or relapse (Supplementary Figure 11), including MS-LCH and SS-multifocal skin disease (Supplementary Figure 9). This insight did not emerge from the study by Héritier *et al.*[10], because the univariable survival analyses presented in their study were only stratified by risk organ involvement – with MS-RO- and SS-multifocal skin disease still overrepresented in *BRAF*^{V600E} mutated patients in the low-risk disease subgroup (Figure 3B). Interestingly, lesional *BRAF*^{V600E} status also did not correlate with inferior clinical outcome in recent molecular studies of adult LCH[31,59–61]. Thus, the quest for independent prognostic factors in LCH continues.

Our study also confirms that *MAP2K1* mutations in pediatric LCH predominantly occur in exon 2, affecting the αA-helix of MEK1 (Figure 5; Supplementary Figure 12)[62,63], with p.Q58_E62del as the most detected mutation (Supplementary Table 9)[19]. The distinction between *MAP2K1* exon 2 or 3 mutations is important, because the mutations in exon 2 are RAF-regulated, whereas the deletions in exon 3 are RAF- and phosphorylation-independent[64]. Consequently, these *MAP2K1* exon 3 deletions are less sensitive to allosteric MEK inhibitors, such as trametinib or cobimetinib[63,64]. Additionally, these so-called "class 3 *MAP2K1* mutants" result in higher activation of downstream ERK *in vitro* when compared to *MAP2K1* exon 2 mutations[64]. Therefore, one could hypothesize that *MAP2K1* exon 3 deletions might associate with a more severe clinical phenotype; however, only 1/17 children in our cohort with these mutations had multisystem LCH (Table 2). In addition, their event-free survival was not significantly worse than of children with *MAP2K1* exon 2 mutations (Supplementary Figure 13). In general, our study points out that *MAP2K1* mutations typically correlate with a less severe clinical presentation of pediatric LCH, with significantly more SS-bone LCH and less multisystem disease compared to *BRAF*^{V600E} (Figure 2).

BRAF exon 12 mutations predominantly comprised small in-frame deletions affecting the β3-αC loop of the BRAF protein (Figure 5; Supplementary Figure 12)[25]. Like in adult LCH[59], *BRAF* p.N486_P490del was the most detected mutation (Supplementary Table 10). Additionally, insertions at the end of *BRAF* exon 12 affecting the αC-β4 loop (Figure 5) were detected in twelve patients[48]. These patients comprised eleven children with the *BRAF* p.R506_K507insLLR mutation, first described in two cases by Héritier *et al.*[28], and one child with a *BRAF* p.L505_R506insTLL mutation. Importantly, both β3-αC and αC-β4 loop mutations are resistant to first-generation BRAF inhibitors like vemurafenib[25,28,46,48]. In accordance with the two cases reported by Héritier *et al.*[28], the αC-β4 loop insertions

predominantly occurred in children with SS-UFB LCH (Table 2). Yet, we also identified this mutation in one child with multisystem LCH that had multiple bone relapses and required four lines of chemotherapy – again demonstrating that (recurrent) mutations are not completely specific to one clinical form of the disease. Interestingly, *BRAF* exon 12 deletions affecting the β3-αC loop seemed to associate with a high prevalence of lung involvement. This is in accordance with molecular studies of adult LCH, which described the frequent presence of these mutations in adult LCH patients with pulmonary involvement[31,59,60] – often in the context of multisystem disease. Thus, molecular analysis of *BRAF* exon 12 should be particularly applied in patients with pulmonary lesions[54,56], which may inform LCH diagnosis and enable rational targeted therapy.

Finally, alternative MAPK pathway gene alterations seemed related to some uncommon disease manifestations, since we observed rare abscess-like soft tissue extension in several *BRAF*^{V600D} mutated patients and atypical solid lung lesions in our case with a *BICD2*::*BRAF* fusion. Notably, all three cases with a *BRAF* fusion had different fusion partners, which stands in contrast to the high prevalence of one specific *ALK* fusion partner (*KIF5B*) in patients with ALK-positive histiocytosis[65]. Thus, comprehensive molecular techniques are essential for detection of these rare genetic variants; their identification may have clinical consequences, as illustrated by our *BICD2*::*BRAF*-positive case that received third-line systemic therapy with trametinib and obtained a complete metabolic response (Supplementary Table 2).

Altogether, these data indicate that oncogenic mutation subtype appears an important – but not the sole – driver of heterogeneity in clinical presentation of pediatric LCH. With increasing access to targeted therapies, identification of the precise somatic driver alteration in patients that could benefit from these agents is important, as mutation subtype influences responsiveness to BRAF and MEK inhibitors. Factors other than mutation subtype seem more involved in driving heterogeneous outcomes within clinical subgroups. To this end, (longitudinal) assessment of mutant alleles in cellular or cell-free DNA derived from peripheral blood and/or bone marrow represents an interesting opportunity for prognostic staging and monitoring response to therapy[66-75].

Why specific mutations associate with distinct LCH clinical presentations remains an interesting and important issue for further investigation[76]. Notably, specific genetic alterations also associate with distinct histiocytic entities[17,65,77], again demonstrating the intimate relationship between molecular pathogenesis and clinical histiocytosis phenotype. Differential ERK activation inflicted by the different genetic alterations may play a role[5,64], although this was not apparent for *MAP2K1* exon 2 vs. exon 3 mutations in our cohort. Additionally, the association of *BRAF*^{V600E} with severe clinical forms of LCH

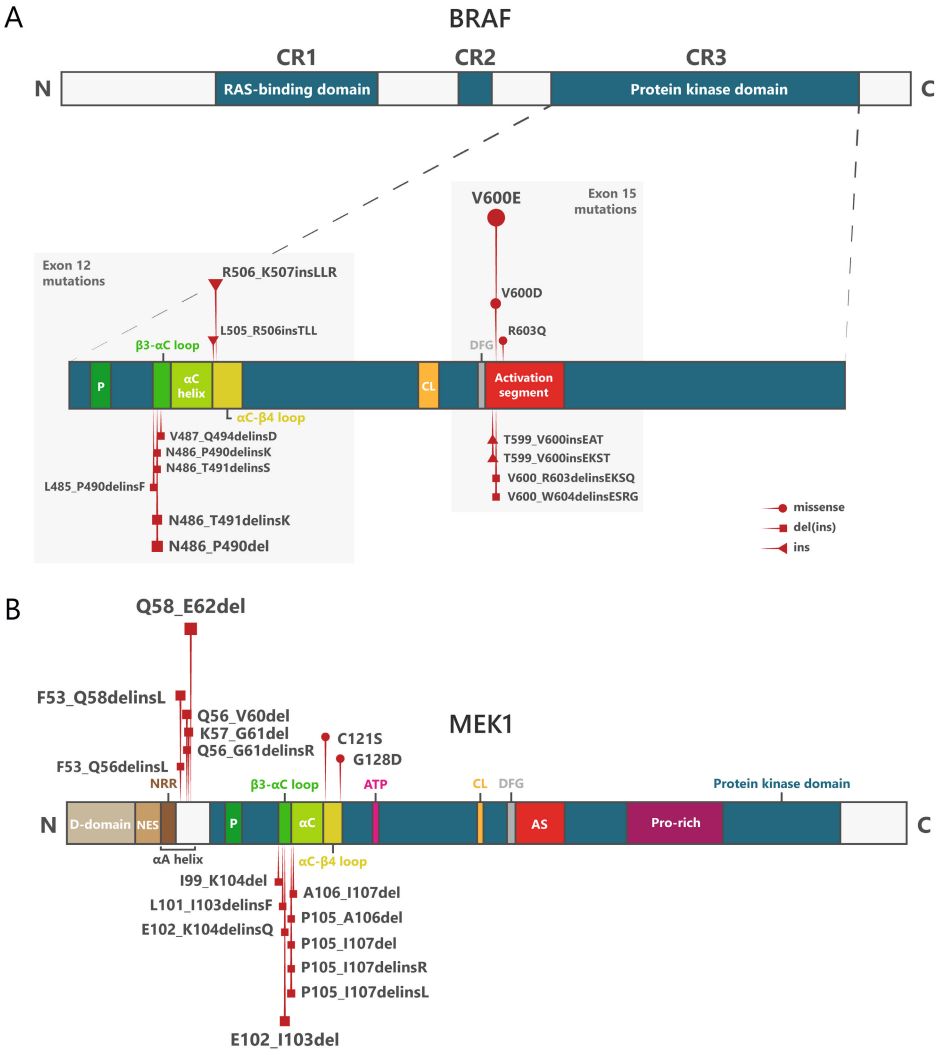

Figure 5. Identified BRAF and MEK1 alterations. (A-B) Schematic representations of BRAF and MEK1 proteins with alterations detected in patients from our cohort. MEK1 is encoded by the gene *MAP2K1*. Figures not entirely to scale. Abbreviations: N, N-terminus; C, C-terminus; CR, conserved region; D, docking; NES, nuclear export signal; NRR, negative regulatory region; P, phosphate-binding; ATP, ATP binding site; CL, catalytic loop; DFG, DFG motif; AS, activation segment; Pro, proline.

may rely on (thus far unknown) mediators or confounders, such as additional (epi) genomic alterations, tissue- or context-specific factors, and the mutated cell-of-origin (Supplementary Figure 11). Although previous whole-exome-sequencing studies have revealed infrequent additional genomic alterations in LCH[17,22,25], several studies have indicated a distinct impact of *BRAF*^{V600E} on the LCH-lesional immune

microenvironment[37,78,79]. Furthermore, several studies have suggested an important role for the mutated cell-of-origin in governing LCH clinical phenotype – with high-risk disease caused by mutations in multipotent hematopoietic stem/progenitor cells and low-risk disease caused by the same mutations in more committed myeloid precursors[16,80,81]. However, also this simplified model does not fully explain LCH clinical phenotype, since recent studies have identified mutation-carrying (myeloid and lymphoid) cells in the blood from patients with low-risk or even single-system LCH[41,80,82]. Therefore, it remains important to elucidate how somatic mutations in multipotent progenitors can cause both single- and multisystemic LCH, and why progenitor cells active in children with high-risk LCH often harbor *BRAF*^{V600E}.

Limitations of our study include the fact that not all *BRAF*^{V600E} negative patients were analyzed beyond *BRAF*^{V600E} (Figure 2A). Consequently, our study does not provide exact incidence rates of *MAP2K1*, *BRAF* exon 12, and rare MAPK pathway gene alterations. However, these alterations were detected in 109 children with LCH, allowing analysis of their clinical associations at unprecedented scale. Furthermore, because of the retrospective design, we cannot rule out some selection bias influencing the clinical spectrum of our cohort. However, our cohort included 288 (76.4%) patients with SS-LCH, compared to <70% in the study by Héritier *et al.*[10], strongly arguing against overrepresentation of patients with severe disease. Instead, we regard the relatively unbiased composition of our cohort as one of the strengths of our study. Nevertheless, our findings should be confirmed by sufficiently powered cohort studies; particularly the potential associations require further investigation (Table 3).

Overall, we present an international clinicogenomic study of childhood LCH, defining the clinical impact of recurrent *BRAF* and *MAP2K1* mutations. We demonstrate distinct associations of these driver mutation subtypes with demographic characteristics, disease extent and specific sites of disease. Another key finding is that mutational status did not associate with event-free survival when patients were stratified by disease extent. These findings advance our understanding of factors underlying the remarkable clinical heterogeneity of pediatric LCH, and may guide molecular diagnostics beyond *BRAF*^{V600E} – e.g. in children with (severe) lung involvement[56].

REFERENCES

1. Maarten Egeler R, van Halteren AGS, Hogendoorn PCW, Laman JD, Leenen PJM. Langerhans cell histiocytosis: fascinating dynamics of the dendritic cell-macrophage lineage. *Immunol. Rev.* 2010;234(1):213–232.
2. Emile J-F, Abla O, Fraitag S, et al. Revised classification of histiocytoses and neoplasms of the macrophage-dendritic cell lineages. *Blood.* 2016;127(22):2672–2681.
3. Allen CE, Beverley PCL, Collin M, et al. The coming of age of Langerhans cell histiocytosis. *Nat. Immunol.* 2020;21(1):1–7.
4. Allen CE, Merad M, McClain KL. Langerhans-Cell Histiocytosis. *N. Engl. J. Med.* 2018;379(9):856–868.
5. Rodriguez-Galindo C, Allen CE. Langerhans cell histiocytosis. *Blood.* 2020;135(16):1319–1331.
6. Lahey ME. Prognostic factors in histiocytosis X. *Am. J. Pediatr. Hematol. Oncol.* 1981;3(1):57–60.
7. Ladisch S, Gadner H. Treatment of Langerhans cell histiocytosis--evolution and current approaches. *Br. J. Cancer. Suppl.* 1994;23:S41-6.
8. Sterlich K, Minkov M. Childhood Langerhans Cell Histiocytosis: Epidemiology, Clinical Presentations, Prognostic Factors, and Therapeutic Approaches. *Rare Dis. - Diagnostic Ther. Odyssey.* 2021; Chapter 4.
9. Haupt R, Minkov M, Astigarraga I, et al. Langerhans cell histiocytosis (LCH): Guidelines for diagnosis, clinical work-up, and treatment for patients till the age of 18 years. *Pediatr. Blood Cancer.* 2013;60(2):175–184.
10. Héritier S, Emile J-F, Barkaoui M-A, et al. BRAF Mutation Correlates With High-Risk Langerhans Cell Histiocytosis and Increased Resistance to First-Line Therapy. *J. Clin. Oncol.* 2016;34(25):3023–3030.
11. Gadner H, Grois N, Pötschger U, et al. Improved outcome in multisystem Langerhans cell histiocytosis is associated with therapy intensification. *Blood.* 2008;111(5):2556–2562.
12. Gadner H, Minkov M, Grois N, et al. Therapy prolongation improves outcome in multisystem Langerhans cell histiocytosis. *Blood.* 2013;121(25):5006–5014.
13. Donadieu J, Bernard F, van Noesel M, et al. Cladribine and cytarabine in refractory multisystem Langerhans cell histiocytosis: results of an international phase 2 study. *Blood.* 2015;126(12):1415–1423.
14. Egeler RM, Katewa S, Leenen PJM, et al. Langerhans cell histiocytosis is a neoplasm and consequently its recurrence is a relapse: In memory of Bob Arceci. *Pediatr. Blood Cancer.* 2016;63(10):1704–1712.
15. Badalian-Very G, Vergilio J-A, Degar BA, et al. Recurrent BRAF mutations in Langerhans cell histiocytosis. *Blood.* 2010;116(11):1919–1923.
16. Berres M-L, Lim KPH, Peters T, et al. BRAF-V600E expression in precursor versus differentiated dendritic cells defines clinically distinct LCH risk groups. *J. Exp. Med.* 2014;211(4):669–683.
17. Durham BH, Lopez Rodrigo E, Picarsic J, et al. Activating mutations in CSF1R and additional receptor tyrosine kinases in histiocytic neoplasms. *Nat. Med.* 2019;25(12):1839–1842.
18. Hayase T, Saito S, Shioda Y, et al. Analysis of the BRAF and MAP2K1 mutations in patients with Langerhans cell histiocytosis in Japan. *Int. J. Hematol.* 2020;112(4):560–567.
19. Yang Y, Wang C, Wang D, et al. Clinical study of MAP2K1-mutated Langerhans cell histiocytosis in children. *J. Cancer Res. Clin. Oncol.* 2022;148(9):2517-2527.

20. Feng S, Han L, Yue M, et al. Frequency detection of BRAF V600E mutation in a cohort of pediatric langerhans cell histiocytosis patients by next-generation sequencing. *Orphanet J. Rare Dis.* 2021;16(1):272.
21. Nelson DS, Quispel W, Badalian-Very G, et al. Somatic activating ARAF mutations in Langerhans cell histiocytosis. *Blood.* 2014;123(20):3152–3155.
22. Chakraborty R, Hampton OA, Shen X, et al. Mutually exclusive recurrent somatic mutations in MAP2K1 and BRAF support a central role for ERK activation in LCH pathogenesis. *Blood.* 2014;124(19):3007–3015.
23. Brown N, Furtado L, Betz B, Kiel M. High prevalence of somatic MAP2K1 mutations in BRAF V600E negative Langerhans cell histiocytosis. *Blood.* 2014;124(10):1655–1659.
24. Nelson DS, van Halteren A, Quispel WT, et al. MAP2K1 and MAP3K1 mutations in langerhans cell histiocytosis. *Genes, Chromosom. Cancer.* 2015;54(6):361–368.
25. Chakraborty R, Burke TM, Hampton OA, et al. Alternative genetic mechanisms of BRAF activation in Langerhans cell histiocytosis. *Blood.* 2016;128(21):2533–2537.
26. Diamond EL, Durham BH, Haroche J, et al. Diverse and Targetable Kinase Alterations Drive Histiocytic Neoplasms. *Cancer Discov.* 2016;6(2):154–165.
27. Lee LH, Gasilina A, Roychoudhury J, et al. Real-time genomic profiling of histiocytoses identifies early-kinase domain BRAF alterations while improving treatment outcomes. *JCI Insight.* 2017;2(3):e89473.
28. Héritier S, Hélias-Rodzewicz Z, Chakraborty R, et al. New somatic BRAF splicing mutation in Langerhans cell histiocytosis. *Mol. Cancer.* 2017;16(1):115.
29. Héritier S, Emile J-F, Hélias-Rodzewicz Z, Donadieu J. Progress towards molecular-based management of childhood Langerhans cell histiocytosis. *Arch. Pédiatrie.* 2019;26(5):301–307.
30. McGinnis LM, Nybakken G, Ma L, Arber DA. Frequency of MAP2K1, TP53, and U2AF1 Mutations in BRAF-mutated Langerhans Cell Histiocytosis. *Am. J. Surg. Pathol.* 2018;42(7):885–890.
31. Jouenne F, Chevret S, Bugnet E, et al. Genetic landscape of adult Langerhans cell histiocytosis with lung involvement. *Eur. Respir. J.* 2020;55(2):1901190.
32. Kemps PG, Hebeda KM, Pals ST, et al. Spectrum of histiocytic neoplasms associated with diverse haematological malignancies bearing the same oncogenic mutation. *J. Pathol. Clin. Res.* 2021;7(1):10–26.
33. Ronceray L, Pötschger U, Janka G, Gadner H, Minkov M. Pulmonary Involvement in Pediatric-Onset Multisystem Langerhans Cell Histiocytosis: Effect on Course and Outcome. *J. Pediatr.* 2012;161(1):129-133. e1-3.
34. Grois N, Pötschger U, Prosch H, et al. Risk factors for diabetes insipidus in langerhans cell histiocytosis. *Pediatr. Blood Cancer.* 2006;46(2):228–233.
35. Grois N, Fahrner B, Arceci RJ, et al. Central Nervous System Disease in Langerhans Cell Histiocytosis. *J. Pediatr.* 2010;156(6):873-881.e1.
36. Chellapandian D, Shaikh F, van den Bos C, et al. Management and Outcome of Patients With Langerhans Cell Histiocytosis and Single-Bone CNS-Risk Lesions: A Multi-Institutional Retrospective Study. *Pediatr. Blood Cancer.* 2015;62(12):2162–2166.
37. Kemps PG, Zondag TC, Steenwijk EC, et al. Apparent Lack of BRAFV600E Derived HLA Class I Presented Neoantigens Hampers Neoplastic Cell Targeting by CD8+ T Cells in Langerhans Cell Histiocytosis. *Front. Immunol.* 2020;10:3045.
38. Melloul S, Hélias-Rodzewicz Z, Cohen-Aubart F, et al. Highly sensitive methods are required to detect mutations in histiocytoses. *Haematologica.* 2019;104(3):e97–e99.

39. van Eijk R, Licht J, Schrumpf M, et al. Rapid KRAS, EGFR, BRAF and PIK3CA Mutation Analysis of Fine Needle Aspirates from Non-Small-Cell Lung Cancer Using Allele-Specific qPCR. *PLoS One*. 2011;6(3):e17791.

40. van Eijk R, Stevens L, Morreau H, van Wezel T. Assessment of a fully automated high-throughput DNA extraction method from formalin-fixed, paraffin-embedded tissue for KRAS, and BRAF somatic mutation analysis. *Exp. Mol. Pathol*. 2013;94(1):121–125.

41. Xiao Y, van Halteren AGS, Lei X, et al. Bone marrow–derived myeloid progenitors as driver mutation carriers in high- and low-risk Langerhans cell histiocytosis. *Blood*. 2020;136(19):2188–2199.

42. Cohen D, Hondelink LM, Solleveld-Westerink N, et al. Optimizing Mutation and Fusion Detection in NSCLC by Sequential DNA and RNA Sequencing. *J. Thorac. Oncol.* 2020;15(6):1000–1014.

43. de Vree PJP, de Wit E, Yilmaz M, et al. Targeted sequencing by proximity ligation for comprehensive variant detection and local haplotyping. *Nat. Biotechnol.* 2014;32(10):1019–1025.

44. Allahyar A, Pieterse M, Swennenhuis J, et al. Robust detection of translocations in lymphoma FFPE samples using targeted locus capture-based sequencing. *Nat. Commun.* 2021;12(1):3361.

45. Schemper M, Smith TL. A note on quantifying follow-up in studies of failure time. *Control. Clin. Trials*. 1996;17(4):343–346.

46. Chen S-H, Zhang Y, Van Horn RD, et al. Oncogenic BRAF Deletions That Function as Homodimers and Are Sensitive to Inhibition by RAF Dimer Inhibitor LY3009120. *Cancer Discov*. 2016;6(3):300–315.

47. Foster SA, Whalen DM, Özen A, et al. Activation Mechanism of Oncogenic Deletion Mutations in BRAF, EGFR, and HER2. *Cancer Cell*. 2016;29(4):477–493.

48. Yap J, Deepak RNVK, Tian Z, et al. The stability of R-spine defines RAF inhibitor resistance: A comprehensive analysis of oncogenic BRAF mutants with in-frame insertion of αC-β4 loop. *Sci. Adv.* 2021;7(24):eabg0390.

49. Ducassou S, Seyrig F, Thomas C, et al. Thymus and mediastinal node involvement in childhood langerhans cell histiocytosis: Long-term follow-up from the French national cohort. *Pediatr. Blood Cancer*. 2013;60(11):1759–1765.

50. Picarsic J, Egeler RM, Chikwava K, Patterson K, Jaffe R. Histologic Patterns of Thymic Involvement in Langerhans Cell Proliferations: A Clinicopathologic Study and Review of the Literature. *Pediatr. Dev. Pathol.* 2015;18(2):127–138.

51. Yao J-F, Wang D, Ma H-H, et al. Characteristics and Treatment Outcomes of Pediatric Langerhans Cell Histiocytosis with Thymic Involvement. *J. Pediatr.* 2022;244(0):194-202.e1-5.

52. Kansal R, Quintanilla-Martinez L, Datta V, et al. Identification of the V600D mutation in Exon 15 of the BRAF oncogene in congenital, benign langerhans cell histiocytosis. *Genes, Chromosom. Cancer*. 2013;52(1):99–106.

53. Janssen LJF, Brons PPT, Schreuder HWB, et al. Image Gallery: A rare abscess-like presentation of Langerhans cell histiocytosis. *Br. J. Dermatol.* 2017;176(4):e33–e33.

54. Kambouchner M, Emile J-F, Copin M-C, et al. Childhood pulmonary Langerhans cell histiocytosis: a comprehensive clinical-histopathological and BRAFV600E mutation study from the French national cohort. *Hum. Pathol.* 2019;89:51–61.

55. Della Valle V, Donadieu J, Sileo C, et al. Chest computed tomography findings for a cohort of children with pulmonary Langerhans cell histiocytosis. *Pediatr. Blood Cancer*. 2020;67(10):e28496.

56. Le Louet S, Barkaoui M-A, Miron J, et al. Childhood Langerhans cell histiocytosis with severe lung involvement: a nationwide cohort study. *Orphanet J. Rare Dis.* 2020;15(1):241.

57. Minkov M, Pötschger U, Thacker N, et al. Additive Prognostic Impact of Gastrointestinal Involvement in Severe Multisystem Langerhans Cell Histiocytosis. *J. Pediatr.* 2021;237:65-70.e1-3.

58. Héritier S, Barkaoui M-A, Miron J, et al. Incidence and risk factors for clinical neurodegenerative Langerhans cell histiocytosis: a longitudinal cohort study. *Br. J. Haematol.* 2018;183(4):608–617.

59. Chen J, Zhao A-L, Duan M-H, et al. Diverse kinase alterations and myeloid-associated mutations in adult histiocytosis. *Leukemia*. 2022;36(2):573-576.

60. Cao X, Duan M, Zhao A, et al. Treatment outcomes and prognostic factors of patients with adult Langerhans cell histiocytosis. *Am. J. Hematol.* 2022;97(2):203–208.

61. Stathi D, Yavropoulou MP, Allen CE, et al. Prevalence of the BRAF V600E mutation in Greek adults with Langerhans cell histiocytosis. *Pediatr. Hematol. Oncol.* 2022;39(6):540-548.

62. Yuan J, Ng WH, Tian Z, et al. Activating mutations in MEK1 enhance homodimerization and promote tumorigenesis. *Sci. Signal.* 2018;11(554):eaar6795.

63. Hanrahan AJ, Sylvester BE, Chang MT, et al. Leveraging Systematic Functional Analysis to Benchmark an In Silico Framework Distinguishes Driver from Passenger MEK Mutants in Cancer. *Cancer Res.* 2020;80(19):4233–4243.

64. Gao Y, Chang MT, McKay D, et al. Allele-Specific Mechanisms of Activation of MEK1 Mutants Determine Their Properties. *Cancer Discov.* 2018;8(5):648–661.

65. Kemps PG, Picarsic J, Durham BH, et al. ALK-positive histiocytosis: a new clinicopathologic spectrum highlighting neurologic involvement and responses to ALK inhibition. *Blood*. 2022;139(2):256-280.

66. Hyman DM, Diamond EL, Vibat CRT, et al. Prospective Blinded Study of BRAF V600E Mutation Detection in Cell-Free DNA of Patients with Systemic Histiocytic Disorders. *Cancer Discov.* 2015;5(1):64–71.

67. Héritier S, Hélias-Rodzewicz Z, Lapillonne H, et al. Circulating cell-free BRAF V600E as a biomarker in children with Langerhans cell histiocytosis. *Br. J. Haematol.* 2017;178(3):457–467.

68. Schwentner R, Kolenová A, Jug G, et al. Longitudinal assessment of peripheral blood BRAFV600E levels in patients with Langerhans cell histiocytosis. *Pediatr. Res.* 2019;85(6):856–864.

69. Eckstein OS, Visser J, Rodriguez-Galindo C, Allen CE. Clinical responses and persistent BRAF V600E+ blood cells in children with LCH treated with MAPK pathway inhibition. *Blood*. 2019;133(15):1691–1694.

70. Donadieu J, Larabi IA, Tardieu M, et al. Vemurafenib for Refractory Multisystem Langerhans Cell Histiocytosis in Children: An International Observational Study. *J. Clin. Oncol.* 2019;37(31):2857–2865.

71. Cui L, Zhang L, Ma H-H, et al. Circulating cell-free *BRAF* V600E during chemotherapy is associated with prognosis of children with Langerhans cell histiocytosis. *Haematologica*. 2020;105(9):e444-447.

72. Wang C-J, Cui L, Ma H-H, et al. BRAF V600E Mutation in Cell-Free DNA, Rather than in Lesion Tissues, at Diagnosis Is An Independent Prognostic Factor in Children with Langerhans Cell Histiocytosis. *Mol. Cancer Ther.* 2021;20(7):1316–1323.

73. Poch R, Le Louet S, Hélias-Rodzewicz Z, et al. A circulating subset of BRAF V600E -positive cells in infants with high-risk Langerhans cell histiocytosis treated with BRAF inhibitors. *Br. J. Haematol.* 2021;194(4):745–749.

74. Eder SK, Schwentner R, Ben Soussia P, et al. Vemurafenib acts as a molecular on-off switch governing systemic inflammation in Langerhans cell histiocytosis. *Blood Adv.* 2022;6(3):970–975.

75. Kudo K, Toki T, Kanezaki R, et al. BRAF V600E-positive cells as molecular markers of bone marrow disease in pediatric Langerhans cell histiocytosis. *Haematologica*. 2022;107(7):1719–1725.

76. McClain KL, Chakraborty R. BRAF V600E vs cell of origin: what governs LCH? *Blood*. 2021;138(14):1203–1204.

77. McClain KL, Bigenwald C, Collin M, et al. Histiocytic disorders. *Nat. Rev. Dis. Prim.* 2021;7(1):73.

78. Zeng K, Wang Z, Ohshima K, et al. BRAF V600E mutation correlates with suppressive tumor immune microenvironment and reduced disease-free survival in Langerhans cell histiocytosis. *Oncoimmunology*. 2016;5(7):e1185582.

79. Sengal A, Velazquez J, Hahne M, et al. Overcoming T-cell exhaustion in LCH: PD-1 blockade and targeted MAPK inhibition are synergistic in a mouse model of LCH. *Blood*. 2021;137(13):1777–1791.

80. Milne P, Bigley V, Bacon CM, et al. Hematopoietic origin of Langerhans cell histiocytosis and Erdheim-Chester disease in adults. *Blood*. 2017;130(2):167–175.

81. Milne P, Abhyankar HA, Scull BP, et al. Cellular distribution of mutations and association with disease risk in Langerhans cell histiocytosis without BRAFV600E. *Blood Adv*. 2022;6(16):4901-4904.

82. Halbritter F, Farlik M, Schwentner R, et al. Epigenomics and Single-Cell Sequencing Define a Developmental Hierarchy in Langerhans Cell Histiocytosis. *Cancer Discov*. 2019;9(10):1406–1421.

83. Zhou X, Edmonson MN, Wilkinson MR, et al. Exploring genomic alteration in pediatric cancer using ProteinPaint. *Nat. Genet*. 2016;48(1):4–6.

84. Cerami E, Gao J, Dogrusoz U, et al. The cBio Cancer Genomics Portal: An Open Platform for Exploring Multidimensional Cancer Genomics Data: Figure 1. *Cancer Discov*. 2012;2(5):401–404.

85. Gao J, Aksoy BA, Dogrusoz U, et al. Integrative Analysis of Complex Cancer Genomics and Clinical Profiles Using the cBioPortal. *Sci. Signal*. 2013;6(269):pl1.

86. Zarnegar S, Durham BH, Khattar P, et al. Novel activating BRAF fusion identifies a recurrent alternative mechanism for ERK activation in pediatric Langerhans cell histiocytosis. *Pediatr. Blood Cancer*. 2018;65(1):e26699.

87. Zanwar S, Abeykoon JP, Dasari S, et al. Clinical and therapeutic implications of BRAF fusions in histiocytic disorders. *Blood Cancer J*. 2022;12(6):97.

88. Zhang R, Wang C-J, Zhao Y-Z, Ma H-H, Wang D, Zhang L, Lian H-H, Li W-J, Zhang Q, Li N, Yang Y, Wang T-Y, Cui L LZ-G. Genetic Landscape and its Prognostic Significance in Children with Langerhans cell Histiocytosis. *Pediatr. Blood Cancer*. 2022;69(S1):e29453.